IOPscience iopscience.iop.org

Home Search Collections Journals About Contact us My IOPscience

Symmetry detection of auxetic behaviour in 2D frameworks

This content has been downloaded from IOPscience. Please scroll down to see the full text.

2013 EPL 102 66005

(http://iopscience.iop.org/0295-5075/102/6/66005)

View the table of contents for this issue, or go to the journal homepage for more

Download details:

IP Address: 129.169.70.162
This content was downloaded on 06/02/2014 at 17:37

Please note that terms and conditions apply.

A Letters Journal Exploring the Frontiers of Physics

June 2013

EPL, **102** (2013) 66005
doi: 10.1209/0295-5075/102/66005

www.epljournal.org

Symmetry detection of auxetic behaviour in 2D frameworks

H. Mitschke[1(a)], G. E. Schröder-Turk[1], K. Mecke[1], P. W. Fowler[2] and S. D. Guest[3]

[1] *Theoretische Physik I, Friedrich-Alexander Universität Erlangen-Nürnberg - Staudtstr. 7, 91058 Erlangen, Germany*
[2] *Department of Chemistry, University of Sheffield - Sheffield S3 7HF, UK*
[3] *Department of Engineering, University of Cambridge - Trumpington Street, Cambridge CB2 1PZ, UK*

received 24 May 2013; accepted in final form 17 June 2013
published online 2 July 2013

PACS 62.20.dj – Poisson's ratio

Abstract – A symmetry-extended Maxwell treatment of the net mobility of periodic bar-and-joint frameworks is used to derive a sufficient condition for auxetic behaviour of a 2D material. The type of auxetic behaviour that can be detected by symmetry has Poisson's ratio -1, with equal expansion/contraction in all directions, and is here termed *equiauxetic*. A framework may have a symmetry-detectable equiauxetic mechanism if it belongs to a plane group that includes rotational axes of order $n = 6$, 4, or 3. If the reducible representation for the net mobility contains mechanisms that preserve full rotational symmetry (A modes), these are equiauxetic. In addition, for $n = 6$, mechanisms that halve rotational symmetry (B modes) are also equiauxetic.

editor's choice Copyright © EPLA, 2013

Introduction. – Auxetic materials (auxetics) have the property that when stretched in one direction they expand in a perpendicular direction, that is, they have a negative Poisson's ratio. Their proposed uses include applications in medical, safety and sensing areas [1–5]. Auxetic deformations are closely related to dilatancy in granular matter [6,7], negative normal stress in biopolymers [8] and the negative Poisson's ratio observed in crumpled crystalline surfaces and membranes [9,10], see also the review [11]. Auxetic properties are known to affect physical properties, such as phonon dispersion and wave propagation or attenuation [12–14]. The focus of many theoretical studies of auxeticity is the identification of mechanisms at the microscopic level that are able to account for the macroscopic behaviour of auxetic (meta-) materials. These typically involve modelling of a structure in terms of a system of hinged rotating rigid polygons [15–17] or, in a complementary approach, as an infinite bar-and-joint framework. The bar-and-joint model has been used to compile a catalogue of planar periodic auxetic tessellations [18–20]. One striking observation that emerges from examination of this catalogue is concerned with the functional form of Poisson's ratio for different 2D auxetic frameworks. There are two distinct patterns. In many cases, Poisson's ratio, ν, the negative of the ratio of transverse to longitudinal strain, is a function of the amount of strain. However, in some cases ν is constant and equal to -1 for all values of strain, the unit cell changes in size but not shape, and the auxetic behaviour for displacement along this mode is isotropic (*equiauxetic*). A material for which Poisson's ratio attains its limiting value of -1 has also been called *maximally auxetic* [21]. Examples of equiauxetic behaviour have been described [22–26]. From the catalogue [18], it is also clear that equiauxetic behaviour is associated with frameworks that have certain symmetries. The catalogue contains examples of equiauxetic frameworks with $p6mm$ symmetry at equilibrium, where the displaced structure retains $p6mm$, $p6$ or $p31m$ symmetry. Other examples have symmetry $p4mm$ or $p4gm$, and retain $p4mm$, $p4gm$ or $p4$ when displaced.

The aim of the present paper is to give a general explanation for these observations, and to derive a symmetry-based sufficient criterion for equiauxetic behaviour of a 2D framework. The treatment is based on Maxwell counting for bar-and-joint and body-and-joint frameworks, extended to take symmetry into account [27], as recently adapted to cover periodic 2D and 3D frameworks [28].

A symmetry basis for equiauxetic behaviour. – The qualitative idea needed to explain the proposed connection between symmetry and equiauxetic behaviour in 2D relies on the fact that the only affine deformation of a continuous body in 2D that has rotational symmetry of order greater than 2 is a uniform expansion/contraction. Consider any deformation mode of the unit cell that

(a) E-mail: holger.mitschke@fau.de (corresponding author)

preserves a rotation axis of order 3 or more. This deformation must be associated with equal strain in all directions, implying a Poisson's ratio of -1 for the mode in question, which hence is equiauxetic.

What can be said about the symmetry of such a deformation mode? In the language of point groups, characters and representations, familiar from Chemistry [29], the mode must belong to an irreducible representation that has character $+1$ under proper rotations $(C_n)^q$ through angles $2\pi q/n$. In fact, this also implies that the mode must be *non-degenerate*, as the kernels and co-kernels for degenerate modes of groups C_{pv} ($p = 6, 4$) preserve at most a C_2 rotational axis (see [30]). This means that all distortions within the space of doubly degenerate E-type vibrations destroy any C_6, C_4, C_3 rotational symmetry.

Candidates for equiauxetic modes are therefore limited to those belonging to irreducible representations of A-type (those having character $+1$ under the principal rotation C_n for $n \geqslant 3$), and B-type (those having character -1 under the principal rotation C_n but $+1$ under $(C_n)^2$). The plane groups (and the point groups isomorphic with their corresponding factor groups) that can support equiauxetic modes are therefore limited to: $p6mm$ (C_{6v}), $p6$ (C_6) (A and B modes); $p4mm$ (C_{4v}), $p4gm$ (C_{4v}), $p4$ (C_4), $p3m1$ (C_{3v}), $p31m$ (C_{3v}), $p3$ (C_3) (A modes). Thus, in the ordering used in the International Tables [31], the "auxetic plane groups" are numbered 10 to 17.

In the following sections, we show how modes of the required types can be identified for microstructured cellular materials, which are appropriately modelled as bar-and-joint [32,33] or body-and-joint frameworks.

Symmetry and mobility of periodic bar-and-joint frameworks in 2D. – It has long been recognised that counting arguments can give powerful conditions for rigidity/mobility of structures. The Calladine extension [34] of Maxwell's rule [35] gives the net mobility $(m - s)$ of a *finite* bar-and-joint 2D framework as

$$m - s = 2j - b - 3, \tag{1}$$

where m is the number of mechanisms, s is the number of states of self-stress of a pin-jointed framework with j joints and b bars, and the constant term accounts for rigid-body motions. The symmetry-extended equivalent of (1) is [27]

$$\Gamma(m) - \Gamma(s) = \Gamma(j) \times \Gamma(T_x, T_y) - \Gamma(b) - \Gamma(T_x, T_y) - \Gamma(R_z), \tag{2}$$

where each representation Γ(object) describes the symmetry of a set of objects (which may be joints, rigid elements, points, vectors or other local structural or dynamical motifs) in the relevant point group of the structure. Γ(object) collects the *characters* $\chi_{\text{object}}(S)$ of sets of objects, *i.e.*, for each symmetry operation S, $\chi_{\text{object}}(S)$ is the trace of the matrix that relates the set before and after the application of S. The rigid-body terms, $\Gamma(T_x, T_y)$ and $\Gamma(R_z)$, are the representations of the in-plane translations and the in-plane rotation, respectively. For further details, see [29].

	Frame (a) Group C_2		Frame (b) Group C_s	
	E	C_2	E	σ
$\Gamma(j)$	6	0	6	0
$\times\Gamma(T_x, T_y)$	2	0	2	0
$=$	12	0	12	0
$-\Gamma(b)$	-9	-1	-9	-3
$-\Gamma(T_x, T_y)$	-2	2	-2	0
$-\Gamma(R_z)$	-1	-1	-1	1
$=\Gamma(m)-\Gamma(s)$	0	0	0	-2

Fig. 1: (Colour on-line) Two bar-and-joint frameworks. Both (a) and (b) comply with the Maxwell rule (1), as expressed in the columns showing how the different representations behave under the trivial identity operation E; in each case the total character given in the final line of the table is zero. The symmetry-extended equation (2) confirms the zero count for (a), where the extra symmetry operation is C_2 and gives no indication of mechanisms or states of self-stress. In case (b) the fact that the total character under the σ-reflection operation is -2 shows that there is at least one mechanism and one state of self-stress. These can be identified as the expected symmetry-breaking mechanism and a totally symmetric state of self-stress.

The terms on the RHS of (2) describe, respectively, the two-dimensional freedoms of the joints, the length constraints enforced by the bars, and the removal of the rigid-body translations and rotation. Each is a generalisation of the corresponding count in (1). Figure 1 shows an example of a simple system for which symmetry provides extra information not available from (1).

The scalar counting rule (1) is the character of the full symmetry equation under the identity operation; it can be extended to *periodic* structures. When proper account is taken of the allowed degrees of freedom of the lattice [36] (stretches and shear motions), the form of (1) appropriate to a periodic system in 2D is [28]

$$m - s = 2j - b + 1. \tag{3}$$

Extending (3) to include periodic symmetry gives [28]

$$\Gamma(m) - \Gamma(s) = \Gamma(j) \times \Gamma(T_x, T_y) - \Gamma(b) + \Gamma_a, \tag{4}$$

where

$$\Gamma_a = \Gamma(T_x, T_y) \times \Gamma(T_x, T_y) - \Gamma(T_x, T_y) - \Gamma(R_z), \tag{5}$$

and all representations Γ are to be calculated in the crystallographic point group isomorphic with the factor group of the full plane group. The representation Γ_a accounts for the difference in symmetry between the three possible deformations of the unit cell and the two allowed rigid-body displacements.

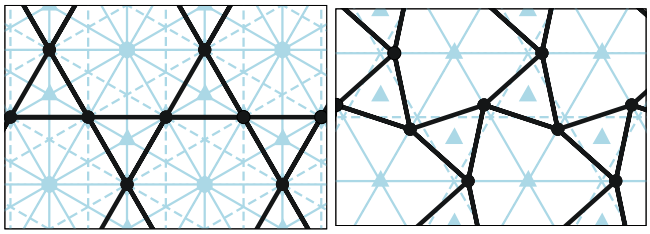

(a) (b)

Fig. 2: (Colour on-line) (a) Kagome framework shown with $p6mm$ symmetry elements; (b) symmetry-detected B_2 mechanism, retaining subgroup $p31m$.

A convenient format for the application of this equation to a periodic framework with some point symmetry is the following tabulation:

C_{6v}	E	$2C_6$	$2C_3$	C_2	$3\sigma_v$	$3\sigma_d$
$\Gamma(j)$	3	0	0	3	1	1
$\times\Gamma(T_x,T_y)$	2	1	−1	−2	0	0
$=$	6	0	0	−6	0	0
$-\Gamma(b)$	−6	0	0	0	−2	0
$+\Gamma_a$	1	−1	1	5	1	1
$\Gamma(m)-\Gamma(s)$	1	−1	1	−1	−1	1

given here for the kagome lattice (fig. 2) with factor group $\mathcal{P}\cong C_{6v}$ in the notation of [37] which makes clear the connection between the point group and the crystallographic plane group, in this case $p6mm$. One obtains $\Gamma(m)-\Gamma(s)=B_2$. The conclusion is that $\Gamma(m)$ contains a mechanism of B_2 symmetry, and there are no symmetry-detectable states of self-stress. The detected mechanism is the known periodic collapse mode for the kagome lattice [38], where alternate triangles rotate in opposite senses, as seen in fig. 2(b). This, in fact, is an auxetic mode.

As an illustration of the additional qualitative information provided by the tabulation, consider the C_2 column in this table. The third entry shows that all six freedoms of the joints are reversed by the C_2 operation; all three points are unshifted by the operation, but it reverses the attached x and y vectors. The entry for $\Gamma(b)$ is zero as all bars are shifted by the operation. The value of 5 for Γ_a arises because the three allowed deformations of the unit cell are symmetric under C_2 but the two rigid-body motions are antisymmetric ($5=+3-(-2)$). The final total of -1 for the character of $\Gamma(m)-\Gamma(s)$ under C_2 tells us that the mechanism that we have detected by using (4) breaks this symmetry of the lattice.

It should be noted that although equations such as (2) and (4) can be powerful in revealing more detail than would be accessible through scalar counting alone, they do have an important limitation in that they necessarily yield only the representation of the relative mobility. If a structure has mechanisms that are equisymmetric with states of self-stress, there will be no evidence for them in $\Gamma(m)-\Gamma(s)$. By definition, then, the mechanisms revealed by (4) are *symmetry-detectable*. The fact that symmetry-detectable mechanisms may become undetectable on descent in symmetry can itself be used to diagnose finite *vs.* infinitesimal mechanisms. The scalar counterpart of detectability is that relationships such as (1) and (3) give only a lower bound on the number of mechanisms.

A criterion for equiauxetic behaviour. – Combination of the reasoning about rotational symmetry of auxetic modes with the symmetry-extended mobility rule (4) leads to the following statement.

Auxeticity criterion: A periodic 2D system with plane group $\mathcal{G}$ and factor group $\mathcal{P}=\mathcal{G}/\mathcal{T}$ has symmetry-detectable equiauxetic behaviour if and only if

1) $\mathcal{P}$ is isomorphic to a point group from the list C_{6v}, C_6, C_{4v}, C_4, C_{3v}, C_3, and

2) the reducible representation $\Gamma(m)-\Gamma(s)$ contains one or more copies of an *auxetic* irreducible representation. The auxetic irreducible representations are: A_1, A_2, B_1, B_2 in C_{6v}; A, B in C_6; A_1, A_2 in C_{4v}; A in C_4; A_1, A_2 in C_{3v}; A in C_3. ($\Gamma(m)-\Gamma(s)$ can be computed according to (4) for bar-and-joint frameworks, and (15) for body-and-joint structures)

For practical calculations it is useful to note the composition of Γ_a within the relevant point groups:

$$\Gamma_a=\begin{cases} A_1\ -E_1\ +E_2 & (C_{6v})\\ A\ \ -E_1\ +E_2 & (C_6)\\ A_1\ +B_1\ +B_2\ -E & (C_{4v})\\ A\ \ +2B\ -E & (C_4)\\ A_1 & (C_{3v})\\ A & (C_3)\end{cases} \tag{6}$$

An alternative way of reaching the same conclusion, in the manner of [39], is to calculate the number of times each auxetic representation occurs in the (reducible) representation $\Gamma(m)-\Gamma(s)$, *i.e.*, to find the coefficients $n(\Gamma_i)$ in the expansion

$$\Gamma(m)-\Gamma(s)=\sum_i n(\Gamma_i)\Gamma_i, \tag{7}$$

where i runs over the irreducible representations of the group. The coefficients $n(\Gamma_i)$ can be found by using well-known projection techniques [29]. It is straightforward to show that the counts for the auxetic representations are: $C_{6v}\cong p6mm/\mathcal{T}$ and $C_{4v}\cong p4mm/\mathcal{T}\cong p4gm/\mathcal{T}$:

$$\begin{aligned} n(A_1)&=2j_1+j_m-(b_1+b_m+b_{2mm})+1,\\ n(A_2)&=2j_1+j_m-\ b_1; \end{aligned} \tag{8}$$

$C_{6v} \cong p6mm/\mathcal{T}$:

$$\begin{aligned} n(B_1) &= 2j_1 + j_m + j_{2mm} - (b_1 + b_{.m.}), \\ n(B_2) &= 2j_1 + j_m + j_{2mm} - (b_1 + b_{..m}); \end{aligned} \tag{9}$$

$C_{3v} \cong p31m/\mathcal{T} \cong p3m1/\mathcal{T}$:

$$\begin{aligned} n(A_1) &= 2j_1 + j_m - (b_1 + b_m) + 1, \\ n(A_2) &= 2j_1 + j_m - b_1; \end{aligned} \tag{10}$$

$C_6 = p6/\mathcal{T}$ and $C_4 = p4/\mathcal{T}$:

$$n(A) = 2j_1 - (b_1 + b_2) + 1; \tag{11}$$

$C_6 = p6/\mathcal{T}$:

$$n(B) = 2(j_1 + j_2) - b_1; \tag{12}$$

$C_3 = p3/\mathcal{T}$:

$$n(A) = 2j_1 - b_1 + 1. \tag{13}$$

Here, the numbers of joints and bars are those in the asymmetric unit of the plane group, subscripted with their (oriented) site symmetry symbol: j_1 and b_1 are in general position; j_2 and b_2 are in special positions having 2-fold rotational symmetry; j_m and b_m are on mirror lines; and j_{2mm} and b_{2mm} are in sites of symmetry $C_{2v} \equiv 2mm$. Dots in (9) are used, in the fashion of [31], where necessary to distinguish settings of the mirror line associated with $C_s \equiv m$.

Symmetry and mobility of periodic body-and-joint structures in 2D. – The scalar and symmetry-extended counting rules developed so far apply to the bar-and-joint model of a repetitive structure. An alternative model is often employed to describe solid-state materials, where the structure is considered as consisting of rigid units connected through flexible joints [40]. For some systems this model may be more appropriate than the use of bars and joints, as will appear below in our treatment of the "TS-wheels" tiling [18,20]. A symmetry-extended counting rule for the mobility of periodic body-and-joint structures has been derived [28] and the auxetic criterion discussed above applies equally to this model.

The model for the 2D case considers the relative degrees of freedom of a repetitive mechanical linkage consisting of unit cells containing n bodies connected by g joints, where in this case each joint permits a single relative rotational freedom. The scalar counting rule is

$$m - s = 3n - 2g + 1, \tag{14}$$

where the RHS expresses the facts that each body has three degrees of freedom in the plane, that each hinge constrains two degrees of freedom, and that the repetitive nature of the system gives the additional single freedom, as discussed above in relation to (3). The symmetry extension of (14) is cast in terms of properties of the "contact polyhedron" C, which is in fact an infinite object, but one for which we need only consider a repeating unit cell. The vertices of C represent the rigid elements, and the edges joints. As described in [28], the symmetry-extended counting rule for this case is

$$\begin{aligned} \Gamma(m) - \Gamma(s) \;=\; & \Gamma(v, C) \times (\Gamma(T_x, T_y) + \Gamma(R_z)) \\ & - \Gamma_{\parallel}(e, C) \times \Gamma(T_x, T_y) + \Gamma_a, \end{aligned} \tag{15}$$

where Γ_a is the same representation as defined in (5).

With the aid of (4) and (15) we now have the conditions for symmetry-detectable equiauxetic mechanisms in both bar-and-joint and body-and-joint structures in 2D.

Examples. – We discuss a number of example frameworks from [18] chosen to illustrate points of particular interest. The names for the various frameworks are those used in the catalogue, supplemented with the symbol for the tiling from [41]. For each example the plane group, the point group, and the net mobility are listed. The examples range from overconstrained, with $m - s$ negative, to underconstrained, with $m - s$ positive. Each is illustrated with a picture showing the framework (in bold) and symmetry elements marked as in the Internationl Tables [31].

Kagome. This is tiling (3.6.3.6), $p6mm$, $6mm(C_{6v})$, $m - s = 1$. The tabular form of the symmetry-adapted mobility calculation was given earlier. With the primitive hexagonal unit cell (fig. 2), scalar counting gives $m - s = 1$, implying the existence of at least one mechanism. The symmetry calculation reveals that this mechanism is equiauxetic (and of B_2 symmetry). As fig. 2(b) shows, the plane group for the deformed configuration is $p31m$, describing a lattice in which each triangle rotates in an opposite sense to its neighbours. Numerical calculations show that the mechanism is unique for the primitive unit cell, in contrast to larger choices with ambiguous modes. These latter contain several paths retaining different symmetries. For instance, application of the given criteria to a framework consisting of 2×2 primitive unit cells gives two equiauxetic modes: the above B_2 mechanism and an additional single A_2 mechanism. Non-equiauxetic modes with $p2gg$ and $p2$ are shown in [38].

TS-wheels. This overconstrained framework is the 2-uniform tiling $(3^6; 3^2.4.3.4)$, $p6mm$, $6mm(C_{6v})$, $m - s = -3$ (fig. 3(a)). Simple counting indicates only the existence of three states of self-stress. Counting with symmetry, as in the tabular calculation

C_{6v}	E	$2C_6$	$2C_3$	C_2	$3\sigma_v$	$3\sigma_d$
$\Gamma(j)$	7	1	1	1	3	1
$\times\Gamma(T_x, T_y)$	2	1	−1	−2	0	0
$=$	14	1	−1	−2	0	0
$-\Gamma(b)$	−18	0	0	0	−4	−2
$+\Gamma_a$	1	−1	1	5	1	1
$\Gamma(m) - \Gamma(s)$	−3	0	0	3	−3	−1

gives $\Gamma(m) - \Gamma(s) = A_2 - A_1 - B_1 - E_1$, implying at least one mechanism, of A_2 symmetry, and four states of self-stress, of symmetries A_1, B_1 and E_1. The detected mechanism corresponds to concerted rotation of the hexagonal "wheels", with simultaneous collapse of the square motifs to flattened rhombi illustrated in fig. 3(b).

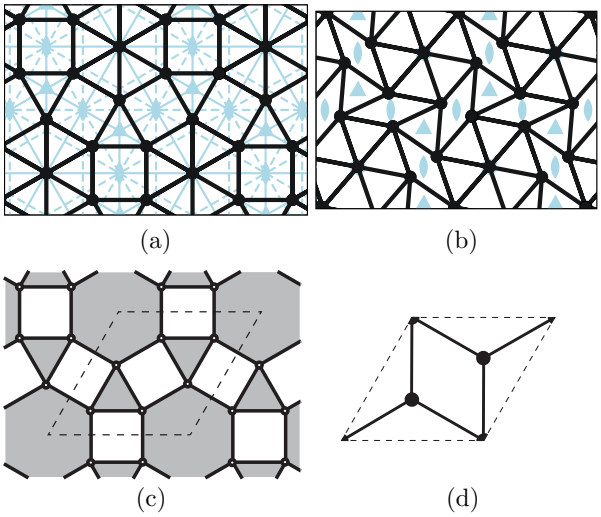

Fig. 3: (Colour on-line) (a) The TS-wheels tiling shown with $p6mm$ symmetry elements; (b) A_2 mechanism retaining $p6$ symmetry; (c) TS-wheels tiling shown as a body-joint model; (d) the contact polyhedron for the body-joint model.

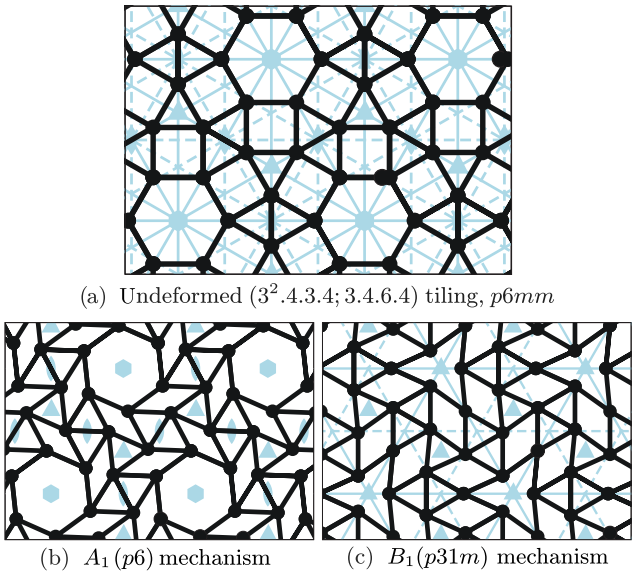

Fig. 4: (Colour on-line) Deformations of the 2-uniform tiling: (b) $A_2(p6)$ mechanism; (c) $B_2(p31m)$ mechanism.

Numerical calculation [20] shows that the symmetry-detected mechanism is the sole mechanism for this choice of unit cell and remains so for larger frameworks composed of $n \times n$ unit cells, for at least $n \leqslant 6$. By its symmetry, this mechanism is equiauxetic. Experimental results for a constructed cellular meta-material with rigid joints, and finite-element simulations of the bar-and-joint framework confirm this prediction of symmetry analysis [19].

The four states of self-stress predicted by symmetry have respective representations A_1, B_1 and E_1; the mechanism would therefore become equisymmetric with the first state of self-stress if followed down from $p6mm$ to $p6$, satisfying a necessary condition for "blocking" of the mechanism, implying that it might be infinitesimal in character rather than finite [42,43]. However, it is easy to see here that the relevant state of self-stress is localised within the hexagonal wheel and cannot block the rotational mechanism. The A_2-symmetric mechanism will continue all the way to the collapsed state where all quadrilaterals have flattened out, yielding a degenerate version of the kagome framework with superimposed bars.

The irrelevance of the "internal" state of self-stress to blocking the mechanism is readily apparent in the alternative body-and-joint model of 2-uniform 5 shown in fig. 3(c). Figure 3(d) shows the contact polyhedron, with vertices corresponding to rigid triangular bodies. A tabular calculation according to (15) is

C_{6v}	E	$2C_6$	$2C_3$	C_2	$3\sigma_v$	$3\sigma_d$
$\Gamma(v,C)$	3	1	3	1	3	1
$\times\Gamma(T_x,T_y,R_z)$	3	2	0	-1	-1	-1
$=$	9	2	0	-1	-3	-1
$-\Gamma_{\parallel}(e,C)$	-6	0	0	0	-2	0
$\times\Gamma(T_x,T_y)$	2	1	-1	-2	0	0
$=$	-12	0	0	0	0	0
$+\Gamma_a$	1	-1	1	5	1	1
$\Gamma(m)-\Gamma(s)$	-2	1	1	4	-2	0

The result $\Gamma(m)-\Gamma(s)=A_2-B_1-E_1$ reveals the same symmetry-detected A_2 mechanism, but now only three states of self-stress, and in particular no state of self-stress that is totally symmetric in $p6mm$. The finite nature of the equiauxetic A_2 mode is therefore apparent from this more physically insightful choice of model structure.

2-uniform tiling 14. This tiling has the description $(3^2.4.3.4;3.4.6.4)$, $p6mm$, $6mm(C_{6v})$, $m-s=-2$. The tiling is illustrated in fig. 4(a) and is included as an example of the possibility of multiple auxetic pathways. The tabular calculation

C_{6v}	E	$2C_6$	$2C_3$	C_2	$3\sigma_v$	$3\sigma_d$
$\Gamma(j)$	12	0	0	0	2	2
$\times\Gamma(T_x,T_y)$	2	1	-1	-2	0	0
$=$	24	0	0	0	0	0
$-\Gamma(b)$	-27	0	0	-3	-5	-1
$+\Gamma_a$	1	-1	1	5	1	1
$\Gamma(m)-\Gamma(s)$	-2	-1	1	2	-4	0

gives the final result $\Gamma(m)-\Gamma(s)=A_2+B_2-A_1-B_1-E_1$, leading to a resolution of the scalar count $m-s$ into a balance of two mechanisms belonging to distinct representations A_2 and B_2 and three states of self-stress belonging to A_1+B_2+E. The two mechanisms correspond to distinct symmetry-reducing pathways, shown in fig. 4(b), (c), with different subgroups of $p6mm$. The A_2 pathway retains $p2$ symmetry, and the B_2 pathway retains centrosymmetric mirror symmetry cm. Both mechanisms are found to be finite [19]. The symmetry results indicate potential blocking of the mechanism by an equisymmetric state of self-stress, but this does not materialise.

Conclusions. – In this work, symmetry considerations have been used to give a basis for understanding generic isotropic auxetic (equiauxetic) mechanisms of

2D materials and meta-materials with sufficiently high symmetry. Explicit criteria for the detection and characterisation of such mechanisms have been given here only for framework models, but could be extended to any model with a well-defined notion of counting degrees of freedom. For symmetric systems, these criteria are often more informative than purely combinatorial approaches. When a system has a unique equiauxetic mode, it will exhibit auxetic behaviour; in the general case, the equiauxetic mode may be accompanied by other modes which may provide alternative non-equiauxetic deformations.

The theory developed here for 2D materials has a 3D counterpart and the necessary symmetry-extended mobility criteria have been given in [28]. In 3D the only affine deformation that preserves cubic symmetry is uniform expansion/contraction. The problem of enumerating 3D systems with equiauxetic modes is challenging, although some constructions are known, see, *e.g.*, fig. 19(b) in [17].

A direction of future exploration beyond the present periodic approach is for materials where local symmetry coexists with long-range disorder. Elastomeric polypropylene films [44] are of this type, and Poisson's ratio and rigidity of random network structures are of interest in several other physical systems [45,46].

* * *

We acknowledge financial support by the DFG through the Engineering of Advanced Materials Cluster of Excellence (EAM) and the research group Geometry and Physics of Spatial Random Systems (GPSRS). PWF acknowledges a Royal Society/Leverhulme Senior Research Fellowship.

REFERENCES

[1] Evans K. E. and Alderson A., *Adv. Mater.*, **12** (2000) 617.
[2] Yang W., Li Z.-M., Shi W., Xie B.-H. and Yang M.-B., *J. Mater. Sci.*, **39** (2004) 3269.
[3] Liu Q., Technical Report, Australian Government, Department of Defence DSTO-GD-0472 (2006).
[4] Alderson A. and Alderson K. L., *Proc. Inst. Mech. Eng. G*, **221** (2007) 565.
[5] Alderson A., *Chem. Ind.* (2011) 18.
[6] Kabla A. J. and Senden T. J., *Phys. Rev. Lett.*, **102** (2009) 228301.
[7] Zhao S.-C., Sidle S., Swinney H. L. and Schröter M., *EPL*, **97** (2012) 34004.
[8] Janmey P. A., McCormick M. E., Rammensee S., Leight J. L., Georges P. C. and MacKintosh F. C., *Nat. Mater.*, **6** (2007) 48.
[9] Boal D. H., Seifert U. and Shillcock J. C., *Phys. Rev. E*, **48** (1993) 4274.
[10] Falcioni M., Bowick M. J., Guitter E. and Thorleifsson G., *Europhys. Lett.*, **38** (1997) 67.
[11] Greaves G. N., Greer A. L., Lakes R. S. and Rouxel T., *Nat. Mater.*, **10** (2011) 823.
[12] Sparavigna A., *Phys. Rev. B*, **76** (2007) 134302.
[13] Koenders M. A. C., *Phys. Status Solidi B*, **246** (2009) 2083.
[14] Ruzzene M. and Scarpa F., *Phys. Status Solidi B*, **242** (2005) 665.
[15] Grima J. N. and Evans K. E., *J. Mater. Sci. Lett.*, **19** (2000) 1563.
[16] Grima J. N., Alderson A. and Evans K. E., *Phys. Status Solidi B*, **242** (2005) 561.
[17] Milton G. W., *J. Mech. Phys. Solids*, **61** (2013) 1543.
[18] Mitschke H., *Deformations of skeletal structures,* Diplomarbeit, Universität Erlangen-Nürnberg (2009).
[19] Mitschke H. *et al.*, *Adv. Mater.*, **23** (2011) 2669.
[20] Mitschke H., Robins V., Mecke K. and Schröder-Turk G. E., *Proc. R. Soc. A*, **469** (2013) 20120545.
[21] Sun K., Souslov A., Mao X. and Lubensky T. C., *Proc. Natl. Acad. Sci. U.S.A.*, **109** (2012) 12369.
[22] Milton G. W., *J. Mech. Phys. Solids*, **40** (1992) 1105.
[23] Grima J. N. and Evans K. E., *Chem. Commun.* (2000) 1531.
[24] Grima J. N., Farrugia P., Caruana C., Gatt R. and Attard D., *J. Mater. Sci.*, **43** (2008) 5962.
[25] Grima J. N., Gatt R., Ellul B. and Chetcuti E., *J. Non-Cryst. Solids*, **356** (2010) 1980.
[26] Grima J. N., Chetcuti E., Manicaro E., Attard D., Camilleri M., Gatt R. and Evans K. E., *Proc. R. Soc. A*, **468** (2012) 810.
[27] Fowler P. W. and Guest S. D., *Int. J. Solids Struct.*, **37** (2000) 1793.
[28] Guest S. D. and Fowler P. W., to be published in *Philos. Trans. R. Soc. A* (2013).
[29] Bishop D. M., *Group Theory and Chemistry* (Oxford University Press) 1973.
[30] McDowell R. S., *J. Mol. Spectrosc.*, **17** (1965) 365.
[31] Wondratschek H. and Müller U. (Editors), *International Tables for Crystallography*, Vol. **A** (International Union of Crystallography, Chester) 2006.
[32] Gibson L. J. and Ashby M. F., *Cellular Solids: Structure and Properties*, 2nd edition (Cambridge University Press, Cambridge) 1997.
[33] Deshpande V. S., Ashby M. F. and Fleck N. A., *Acta Mater.*, **49** (2001) 1035.
[34] Calladine C. R., *Int. J. Solids Struct.*, **14** (1978) 161.
[35] Maxwell J. C., *Philos. Mag.*, **27** (1864) 294.
[36] Guest S. D. and Hutchinson J. W., *J. Mech. Phys. Solids*, **51** (2003) 383.
[37] Burns G. and Glazer A. M., *Space Groups for Solid State Scientists* (Academic Press, Inc.) 1978.
[38] Kapko V., Treacy M. M. J., Thorpe M. F. and Guest S. D., *Proc. R. Soc. A*, **465** (2009) 3517.
[39] Connelly R., Fowler P. W., Guest S. D., Schulze B. and Whiteley W. J., *Int. J. Solids Struct.*, **46** (2009) 762.
[40] Giddy A. P., Dove M. T., Pawley G. S. and Heine V., *Acta Crystallogr.A*, **49** (1993) 697.
[41] Grünbaum B. and Shephard G. C., *Tilings and Patterns* (W. H. Freeman and Company, New York) 1987.
[42] Kangwai R. D. and Guest S. D., *Int. J. Solids Struct.*, **36** (1999) 5507.
[43] Guest S. D. and Fowler P. W., *J. Mech. Mater. Struct.*, **2** (2007) 293.
[44] Franke M. and Magerle R., *ACS Nano*, **5** (2011) 4886.
[45] Bhaskar A., *EPL*, **87** (2009) 18004.
[46] Delaney G. W., Weaire D. and Hutzler S., *Europhys. Lett.*, **72** (2005) 990.